

Surface reactions of monoethylgermane on Si(100)-(2 × 1)

Lori A. Keeling¹, Li Chen², C. Michael Greenlief*

Department of Chemistry, University of Missouri–Columbia, Columbia, MO 65211, USA

Received 17 June 1997; accepted for publication 20 October 1997

Abstract

The adsorption and decomposition of monoethylgermane (GeH_3Et) on the Si(100)-(2 × 1) surface was investigated with the intent of elucidating the surface processes leading to the deposition of germanium. The low-temperature adsorption of the molecule was explored, as well as its thermal decomposition. H_2 and C_2H_4 are observed as the desorption products in temperature-programmed desorption experiments. The ethylene is produced by a hydride elimination reaction within the adsorbed ethyl groups. The amount of Ge which can be deposited in a reaction cycle is correlated with the number of sites occupied by the ethyl groups upon the dissociation of GeH_3Et . © 1998 Elsevier Science B.V.

Keywords: Chemical vapor deposition; Ethylgermane; Photoelectron spectroscopy; Silicon; Surface decomposition reactions; Thermal desorption spectroscopy

1. Introduction

The silicon–germanium system has become increasingly important because of its potential applications in electronic devices [1–7]. Digermane (Ge_2H_6) and germane (GeH_4) are the two most common germanium-containing molecular precursors which are used in the chemical vapor deposition (CVD) of Ge [8–20]. However, these two gases are pyrophoric, and their handling and disposal are important safety concerns. With these concerns in mind, there is interest in the development of alternative precursors for germanium. Alkylgermanes such as monoethylgermane

(GeH_3Et) are possible substitutes. GeH_3Et is a liquid near room temperature with a vapor pressure suitable for CVD, is less reactive with air, and is easier to handle than conventional hydride sources.

There are several published studies examining the interactions of ethylgermanes and ethylsilanes with a variety of Si surfaces [21–35]. The adsorption and decomposition of GeH_2Et_2 has been investigated previously [35]. The low-temperature adsorption behavior of GeH_2Et_2 was examined by ultraviolet photoelectron spectroscopy (UPS). It was observed that GeH_2Et_2 adsorbs dissociatively on the surface. The adsorption products are GeH_2 and adsorbed ethyl groups at low coverages and a surface temperature of 110 K. At coverages greater than $7.5 \times 10^{13} \text{ cm}^{-2}$, GeH_2Et_2 physisorbs on top of the dissociated layer. Annealing the surface to higher temperatures results in the decomposition of the adsorbed ethyl groups and

* Corresponding author. Fax: (+1) 573 8822754;
e-mail: chemcmg@showme.missouri.edu

¹ Present address: Panasonic/MASCA, 1111 39th Ave, S.E., Puyallup, WA 98374, USA.

² Present address: Monsanto Company, 800 N. Lindbergh Blvd., St. Louis, MO 63167, USA.

GeH₂. GeH₂ decomposes to GeH with a hydrogen atom transferring to the silicon surface by 150 K. Atomic Ge is produced when the GeH group decomposes at temperatures greater than 150 K. The ethyl groups decompose and produce ethylene by a hydride elimination reaction over the temperature range 600–750 K. The final reaction products are H₂, C₂H₄ and atomic Ge. H₂ and C₂H₄ are observed in temperature-programmed desorption (TPD) experiments. Hydrogen desorption is dominated by a single desorption peak at 800 K. The desorption of ethylene has a peak maximum near 700 K. The surface after GeH₂Et₂ exposure and H₂ and C₂H₄ desorption was free from carbon contamination. These studies were also consistent with the room-temperature adsorption studies of GeH₂Et₂ by Coon et al. on the Si(111)-(7×7) surface [27,29,31,32].

Mahajan and co-workers have explored the surface chemistry of SiH₂Et₂ and GeH₂Et₂ on Si(100) using high-resolution electron energy loss spectroscopy (HREELS) and TPD [25]. Both SiH₂Et₂ and GeH₂Et₂ adsorbed dissociatively at the Si surface for room-temperature exposures, producing adsorbed ethyl groups and hydrogen atoms. H₂ and C₂H₄ were detected as desorption products. The authors reported that the Ge–C stretching mode was observed rather than the Si–C stretching mode from GeH₂Et₂-exposed surfaces in HREEL spectra at room temperature. They suggested that the ethyl groups remained bound to Ge atoms during the decomposition of GeH₂Et₂, and that the ethyl groups do not migrate from Ge to Si sites prior to or during the desorption of ethylene.

Foster et al. investigated the adsorption and reactions of monoethylsilane (SiH₃Et) on Si(100) using HREELS and TPD [24]. SiH₃Et adsorbed dissociatively at room temperature on Si(100). The vibrational modes associated with the ethyl ligands disappeared in HREELS experiments and the vibrational modes for the Si–H bond increased in intensity as the crystal temperature was raised. This observation was attributed to the transfer of hydrogen to the surface as the ethyl groups underwent hydride elimination to produce gas-phase C₂H₄. These results are qualitatively similar to those of Schmidt et al. [22] and Coon et al. [31].

In an effort to further understand the surface

processes leading to germanium deposition, the low-temperature adsorption of GeH₃Et on the Si(100)-(2×1) surface is investigated. The position and identification of the ethylgermane molecular orbitals on Si(100)-(2×1) is aided by ab-initio calculations. The eventual thermal decomposition products are molecular hydrogen, ethylene and adsorbed germanium. TPD is used in combination with photoelectron spectroscopy to monitor the surface processes.

2. Experimental

The experiments were conducted in a stainless-steel ultrahigh vacuum chamber. The chamber was equipped with a double-pass cylindrical mirror analyzer (CMA) for Auger electron and photoelectron spectroscopies, a differentially pumped ultraviolet discharge lamp, a twin X-ray source, an ion gun and a quadrupole mass spectrometer for both temperature-programmed desorption and secondary ion mass spectrometry. The base pressure of the system was 6×10^{-11} Torr with a typical working pressure of 1×10^{-10} Torr.

Samples were cleaved into 10 mm × 25 mm × 0.4 mm rectangles from n-type Si(100) wafers (Virginia Semiconductor, ±0.25° of the (100) plane, Sb-doped, 5–10 mΩ·cm resistivity) and mounted to a liquid-nitrogen cooled manipulator. The sample was held by molybdenum clamps for resistive heating. The sample temperature was monitored by a pair of chromel–alumel thermocouples attached to the back of the sample with Aremco 516 ceramic adhesive.

Surface cleanliness was followed by Auger electron and ultraviolet photoelectron spectroscopies. A clean surface was generated by the removal of the native oxide by repeated heating to 1213 K in vacuum followed by slow cooling to room temperature.

Monoethylgermane was synthesized by NaBH₄ reduction of trichloroethylgermane (GeCl₃Et) at a reduced pressure (400 Torr) using a procedure originally proposed by Griffiths [36]. The purity of the GeH₃Et was checked by proton NMR, gas chromatography and in-situ mass spectrometry. The product was further purified by several freeze–

pump–thaw degassing cycles prior to introduction to the UHV chamber. The gas was admitted to the chamber through an effusive doser and directed onto the front face of the crystal at an apparent pressure of 3×10^{-10} Torr above the base pressure for various periods of time. The surface temperature during the exposures was 110 K. The temperature ramp rate used in the TPD experiments was 6 K s^{-1} . The surface coverages were measured by either X-ray photoelectron spectroscopy or H_2 thermal desorption. The H_2 thermal desorption area was used to determine the coverage of the adsorbed gas, as described previously [37].

X-ray photoemission spectra were taken with Al $K\alpha$ radiation (1486.6 eV) with the anode operating at a power of 435 W. The CMA was operated at a fixed pass energy of 25 eV. The Si 2p transition for the clean Si surface was measured at a binding energy of 99.4 ± 0.1 eV.

Ultraviolet photoemission spectra were taken with He II radiation (40.8 eV) from a He gas discharge lamp, and the CMA was operated at a fixed pass energy of 20 eV. All the reported binding energies are referenced to the Si valence band edge, which is assigned as 0 eV binding energy.

Ab-initio molecular orbital calculations were performed with the GAUSSIAN92 system [38] using a modified double-zeta effective core potential basis set (Los Alamos National Laboratories 1-double zeta, LANL1DZ [39–41]). The basis set was modified by the addition of 5d orbitals for Ge which allow for the polarization of electron density. All equilibrium geometries and transition-state geometries were fully optimized at the Hartree–Fock (HF) level. Vibrational frequencies and zero point energies were obtained from the analytical second derivatives [42] calculated at the HF/LANL1DZ level using the HF/LANL1DZ optimized geometries.

3. Results

3.1. Photoemission results

The low-temperature adsorption behavior of GeH_3Et was examined by ultraviolet photoelectron spectroscopy (UPS). Fig. 1 shows the He II UPS

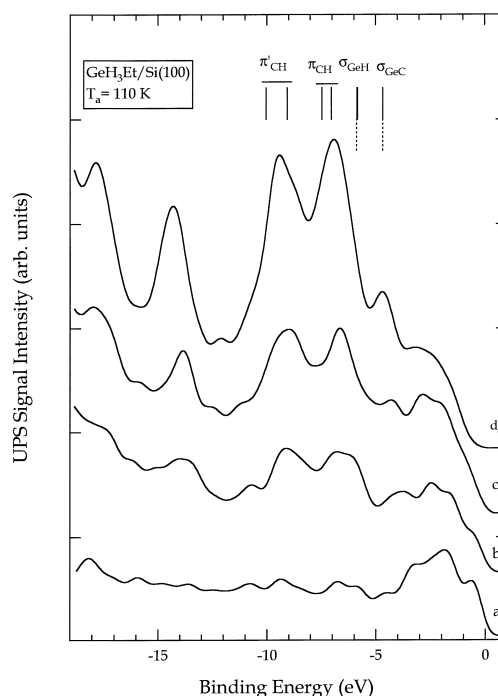


Fig. 1. He II UPS spectra for various exposures of GeH_3Et to Si(100) at 110 K. The spectrum of the clean Si surface is shown as spectrum a. The GeH_3Et coverages shown are (b) 3.7×10^{13} , (c) 5.5×10^{13} and (d) 1.4×10^{14} GeH_3Et molecules per cm^2 .

spectra for several different coverages of GeH_3Et exposed to Si(100) at a surface temperature of 110 K. The He II photoelectron spectrum of the clean Si(100) surface is included (Fig. 1a) for reference. The UPS spectrum for a GeH_3Et coverage of $1.4 \times 10^{14} \text{ cm}^{-2}$ is shown as Fig. 1d, and at this coverage molecular GeH_3Et is observed as a desorption product (see below). The bar graphs at the top of the Fig. 1 are used to help assign the features in the spectrum. The two dashed lines are the energies obtained from the gas-phase photoelectron spectrum of GeH_3Et [43]. The dashed line for the lowest energy peak from the gas-phase spectrum (highest occupied molecular orbital) is aligned with the peak at 4.7 eV binding energy in Fig. 1d. The bar graph with the solid lines at the top of Fig. 1 is the calculated molecular orbital energies for gas-phase GeH_3Et assuming that Koopmans' theorem [44] is obeyed in the photoelectron experiment. The highest occupied molecu-

lar orbital in the calculated spectrum is also aligned with the peak at 4.7 eV. Based on the agreement between the calculated and gas-phase data and the observation of molecular GeH_3Et desorption for this coverage, we conclude that the spectrum presented as Fig. 1d is that of physisorbed GeH_3Et . Using the assignments in the previously measured gas-phase spectrum [43] and a population analysis of the calculated spectrum, the UPS spectrum of physisorbed GeH_3Et can be assigned as follows, using the symmetry notation of Jorgensen and Salem [45]: 4.7 eV, σ_{GeC} ; 5.9 eV, σ_{CGeH} ; 6.9 eV, π_{CH_3} ; 9.4 eV, π'_{CH_3} ; 11.4 eV, σ_{GeH} ; 14.3 eV, σ_{CC} ; and 17.8 eV, C 2s.

Having made the assignments for physisorbed GeH_3Et , consider the lower coverages shown as Fig. 1b and 1c. Fig. 1b is the UPS spectrum obtained from an initially clean Si(100) surface exposed to GeH_3Et at a surface temperature of 110 K. The resulting coverage is $3.7 \times 10^{13} \text{ cm}^{-2}$. Spectrum 1c is the same type of experiment, except that the GeH_3Et coverage is $5.5 \times 10^{13} \text{ cm}^{-2}$. Several changes are observed in the UPS spectra as the GeH_3Et coverage is altered. Between 5 and 10 eV binding energy, the peaks associated with the ethyl groups are considerably broader and at the lowest coverages (Fig. 1b), multiple sets of peaks are present, but not resolved. At about 3 eV in Fig. 1b and 1c, a new peak is observed which is not present in the multilayer spectrum. There are also small binding-energy shifts for the main spectral features with exposure.

The adsorption of GeH_3Et was also followed by XPS, and these results are presented in Fig. 2. The $\text{Ge } 2p_{3/2}$ XPS signal intensity is plotted versus binding energy for several GeH_3Et coverages at a surface temperature of 110 K. The intensity of the $\text{Ge } 2p_{3/2}$ peak increases smoothly with increasing GeH_3Et coverage. The coverage dependence of the $\text{Ge } 2p_{3/2}$ binding energy is shown as an inset to Fig. 2. The binding energy of the peak increases by 0.5 eV over the range of coverages examined.

Additional photoelectron spectroscopy experiments were performed as a function of surface temperature. Fig. 3 shows the results from a series of annealing experiments as examined by UPS. Fig. 3a is the UPS spectrum for a coverage of $5.5 \times 10^{13} \text{ GeH}_3\text{Et}$ molecules per cm^2 at a surface

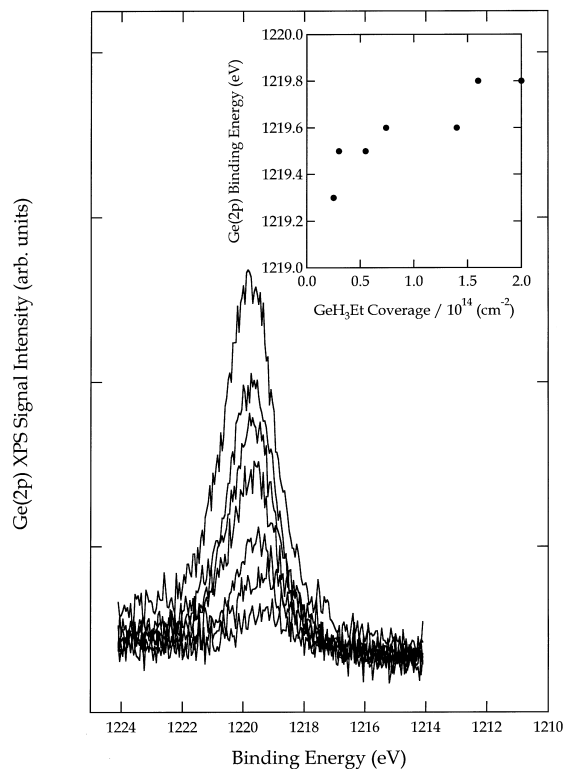


Fig. 2. $\text{Ge } 2p_{3/2}$ XPS signal versus binding energy for several GeH_3Et coverages. The adsorption temperature is 110 K. The coverages shown are (a) 2.5×10^{13} , (b) 3.0×10^{13} , (c) 5.5×10^{13} , (d) 7.4×10^{13} , (e) 1.4×10^{14} , (f) 1.6×10^{14} and (g) 2.0×10^{14} GeH_3Et molecules per cm^2 . Inset: $\text{Ge } 2p_{3/2}$ binding energy as a function of GeH_3Et coverage. Each point is the average of at least three replicate experiments.

temperature of 110 K. Fig. 3b shows the results of heating the GeH_3Et -covered silicon surface to 309 K and cooling to 110 K before recording the UPS spectrum. Fig. 3c was obtained after heating the surface to 503 K, and Fig. 3d is the spectrum obtained after heating to 703 K. Upon heating to 309 K there are minor changes in the UPS spectrum compared to that obtained at 110 K. The most significant change occurs in the peak near 15 eV binding energy, where there is a pronounced shoulder to the higher energy side. However, the majority of the spectral features are associated with molecular GeH_3Et . Heating to 503 K results in the disappearance of the peak at 4.4 eV which is due the σ_{GeC} bonding molecular orbital (in Fig. 3a). The spectrum of the surface annealed to

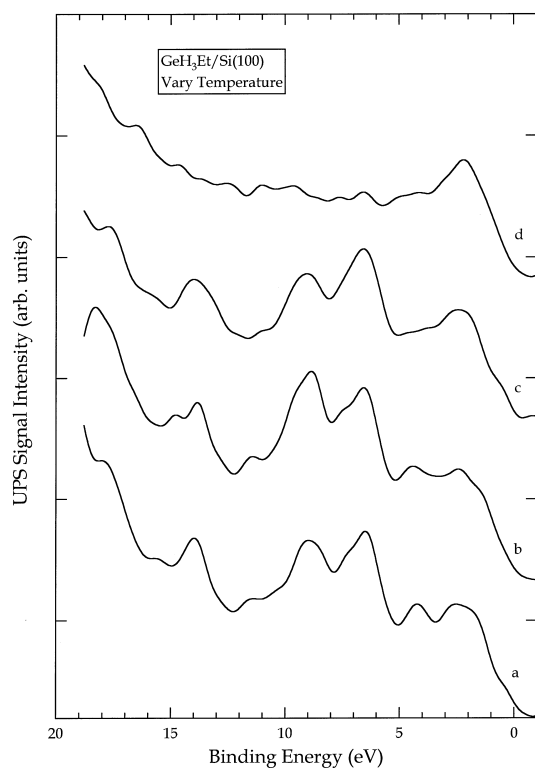


Fig. 3. He II UPS spectra of a GeH₃Et-covered Si(100) surface annealed to various temperatures. The initial adsorption temperature was 110 K. The annealing temperatures shown are (a) 110, (b) 309, (c) 503 and (d) 703 K. The initial GeH₃Et coverage was 5.5×10^{13} molecules per cm², and the spectra were recorded at 110 K.

503 K is representative of that obtained for ethyl groups adsorbed on Si(100) [35,46,47]. Further heating to 703 K results in the disappearance of most of the spectral features.

Fig. 4 shows the corresponding XPS results for a similar set of annealing experiments at the same coverage as shown in Fig. 3. The Ge 2p_{3/2} signal intensity is plotted versus binding energy for several different annealing temperatures. Fig. 4a is the Ge 2p_{3/2} XPS spectrum for an initial GeH₃Et coverage of 5.5×10^{13} cm⁻² at a surface temperature of 110 K. The single peak is centered at 1219.4 eV binding energy. Heating the surface to 309 K, cooling to 110 K and then recording the XPS spectrum yields the results shown as Fig. 4b. The resulting peak shifts to lower binding energy and the full width at half maximum (FWHM)

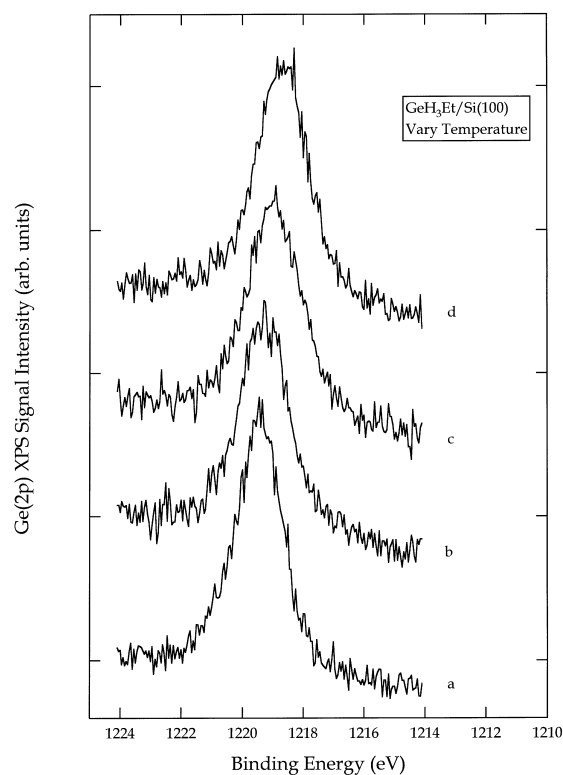


Fig. 4. Ge 2p_{3/2} XPS signal versus binding energy for a GeH₃Et-covered Si(100) surface annealed to various temperatures. The initial adsorption temperature was 110 K. The annealing temperatures shown are (a) 110, (b) 309, (c) 517 and (d) 700 K. The initial GeH₃Et coverage was 5.5×10^{13} molecules per cm², and the spectra were recorded at 110 K.

also increases. Warming the surface to 517 K (Fig. 4c) causes the Ge 2p transition to shift again to lower energies with a broadening of the FWHM. Annealing the surface to 700 K (Fig. 4d) results in a final binding energy of 1218.6 eV.

3.2. Temperature-programmed desorption results

The adsorption and decomposition of GeH₃Et was also followed by TPD. The only desorption products observed by TPD at all coverages were H₂ and C₂H₄. For initial GeH₃Et coverages greater than 7.4×10^{13} cm⁻², molecular GeH₃Et desorption is also observed. Fig. 5 and Fig. 6 summarize the results of several TPD experiments. No carbon is observed on the Si surface within the detection

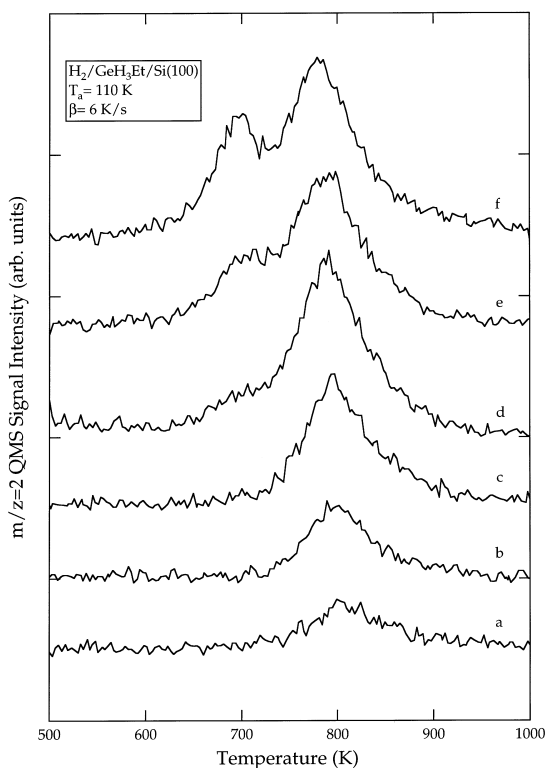


Fig. 5. TPD spectra of H_2 following different exposures of GeH_3Et at a surface temperature of 110 K. The initial GeH_3Et coverages shown are (a) 2.5×10^{13} , (b) 3.7×10^{13} , (c) 5.5×10^{13} , (d) 7.4×10^{13} , (e) 1.6×10^{14} and (f) 2.0×10^{14} molecules per cm^2 .

limits of AES after the temperature ramp in these TPD experiments.

The H_2 desorption results from the decomposition of GeH_3Et are shown in Fig. 5. The H_2 desorption spectra at low coverages (Fig. 5a–c) are dominated by a single desorption feature centered near 800 K. As the coverage is increased above $7 \times 10^{13} \text{ cm}^{-2}$, a second desorption state is observed near 700 K. A large contribution to the desorption state at 700 K is due to the fragmentation of C_2H_4 in the ionization region of the mass spectrometer (see below). However, some of the desorption intensity at 700 K is from the β_2 hydrogen desorption state reported previously on $\text{Si}(100)$ [48].

Fig. 6 presents the ethylene desorption signal from the decomposition of GeH_3Et for several different initial coverages. The C_2H_3^+ ion intensity

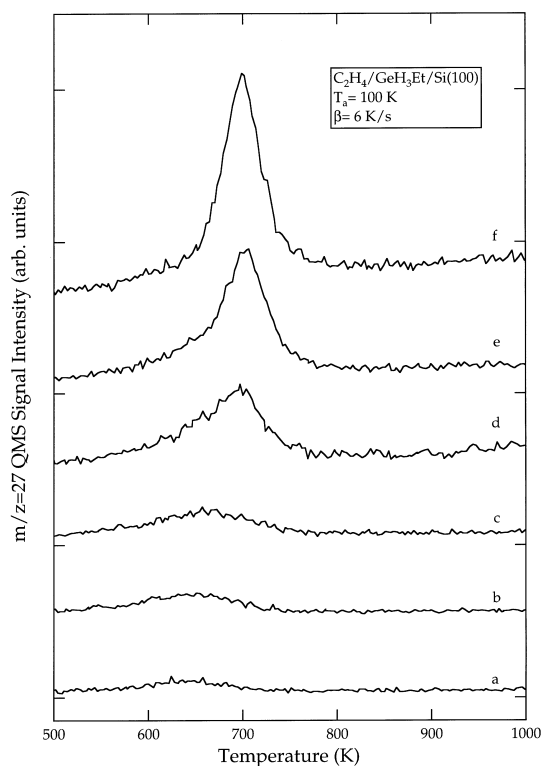


Fig. 6. TPD spectra of C_2H_4 following different exposures of GeH_3Et at a surface temperature of 100 K. The initial GeH_3Et coverages shown are (a) 2.5×10^{13} , (b) 3.7×10^{13} , (c) 5.5×10^{13} , (d) 7.4×10^{13} , (e) 1.6×10^{14} and (f) 2.0×10^{14} molecules per cm^2 .

was followed in TPD experiments to allow for a better discrimination against background signals in the UHV chamber. At the lowest GeH_3Et coverages (Fig. 6a), a single broad C_2H_4 desorption peak is observed at 640 K. The C_2H_4 desorption state increases in intensity with increasing GeH_3Et exposures up to a coverage of $2 \times 10^{14} \text{ cm}^{-2}$. The peak temperature of the state initially observed at 640 K also shifts toward higher temperatures with increasing GeH_3Et coverage. The maximum peak temperature is 700 K for an initial coverage of $1.6 \times 10^{14} \text{ cm}^{-2}$ (Fig. 6e). The peak area for the desorption state at 700 K remains constant for coverages greater than $2.6 \times 10^{14} \text{ cm}^{-2}$, and this is interpreted as being due to a maximum amount of GeH_3Et which will decompose on the $\text{Si}(100)$ surface.

There is also a low-temperature C_2H_4 desorption

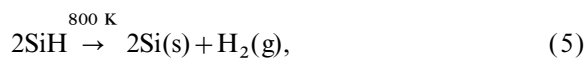
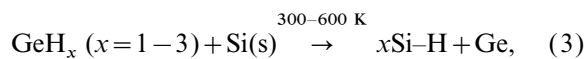
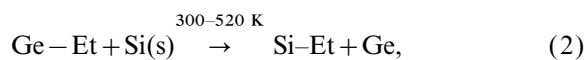
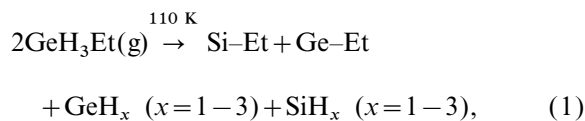
state which has a peak temperature of 140 K (not shown in Fig. 6). The position of the desorption peak does not shift in temperature with exposures greater than $7.4 \times 10^{13} \text{ cm}^{-2}$, and its intensity does not saturate with increasing exposures. This low-temperature state is attributed to the desorption of physisorbed GeH_3Et , which fragments in the ionization region of the mass spectrometer to yield C_2H_4 .

The assignment of the low-temperature C_2H_4 desorption state to physisorbed GeH_3Et was confirmed by monitoring the $m/z = 103$ fragmentation ion (GeH_2Et^+) for molecular GeH_3Et . In these TPD experiments, a single desorption state is observed at a temperature of 140 K and the state is observed only when the coverage exceeds $7.4 \times 10^{13} \text{ cm}^{-2}$. Based on the C_2H_4 TPD results and the fragmentation pattern of GeH_3Et , it is clear that the desorption state at 140 K corresponds to physisorbed GeH_3Et .

4. Discussion

The results presented here demonstrate that Ge can be deposited onto the Si(100) surface by the thermal decomposition of GeH_3Et . The maximum amount of Ge that can be deposited from a saturation exposure of GeH_3Et is 0.38 ML or 2.6×10^{14} Ge atoms per cm^2 .

Before discussing details and before comparing this study with earlier work, we present below a plausible mechanism for the decomposition processes.



where (g) designates a gas-phase species, (s) denotes a surface species, and the remaining intermediates are adsorbed species.

In the first step of the proposed mechanism, GeH_3Et is exposed to the Si(100) surface at low temperature, which results in dissociative adsorption. This reaction step was followed in UPS experiments. As shown in Fig. 1, for low exposures of GeH_3Et there are spectral features which cannot be explained as being solely due to molecular adsorption. The peak at 3.8 eV can be attributed to surface silicon-hydride groups [49–52]. Germanium hydrides are observed at higher binding energies [33,53–55]. Between 5 and 10 eV binding energy are the molecular orbitals associated with surface ethyl groups [35,46,47]. Recent model calculations for adsorbed ethyl groups on Si and Ge sites revealed a binding-energy difference of 0.5 eV in molecular orbital energies for the two systems [56]. This separation in energy is not sufficient to be observed as two clearly resolved peaks with the current experimental set-up. However, the difference in energy is observed as an increase in the overall width of the spectral features, as seen in Fig. 1b. This is interpreted as dissociative adsorption of GeH_3Et , where the ethyl groups are bound to both Si and Ge. The exact composition of the surface hydrides cannot be determined in this study because of the spectral overlap of the silicon and germanium hydride features. As the exposure is increased, GeH_3Et can physisorb on top of the dissociated layer, so that by a coverage of $2.6 \times 10^{14} \text{ cm}^{-2}$, the UPS spectrum is dominated by physisorbed GeH_3Et and the peaks between 5 and 10 eV in the UPS spectra narrow in width.

In the second step of the reaction sequence, surface ethyl groups initially bound to Ge transfer to surface Si sites. This transfer is observed by both X-ray and ultraviolet photoelectron spectroscopy (Fig. 3 and Fig. 4). Heating the GeH_3Et -exposed surface to 503 K results in a UPS spectrum where the binding energy of the peaks associated with the ethyl groups are observed at the same binding energy as ethyl groups adsorbed on Si(100) generated by the decomposition of $\text{C}_2\text{H}_5\text{Br}$ [46,47]. The remaining peaks in the spectrum can be attributed to a mixture of silicon

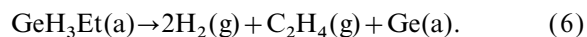
and germanium hydrides. In analogous XPS annealing experiments, heating a GeH₃Et-covered surface to 517 K led to a decrease in binding energy of Ge 2p by 0.4 eV. The decrease in binding energy is consistent with a Ge environment which is becoming more atomic in nature.

In Eq. (3), surface germanium hydrides decompose by the transfer of hydrogen to surface Si sites. The reaction takes place without the desorption of hydrogen, as observed in TPD experiments. The changes in the 2–5 eV binding energy region of UPS spectra, such as Fig. 3b and 3c, also reflect these changes in surface hydrides. This type of transfer is also consistent with that observed previously in the literature [57–59].

Eq. (4) shows the decomposition of surface ethyl groups by hydride elimination to form the desorption product (ethylene). Ethylene desorption occurs in a single desorption state with a peak maximum at 650–700 K, depending on the initial GeH₃Et exposure. The ethylene desorption temperature is consistent with desorption from Si sites, as reported previously [21–35], whereas ethyl groups decompose to ethylene and desorb at 650 K from Ge(100) and the peak temperature is independent of coverage [26,60].

In the final step of the above mechanism, surface silicon hydrides decompose to form molecular hydrogen. The desorption temperature of the hydrogen is the same as that normally observed on Si(100) [48]. The above reaction sequence is also similar to what has been proposed for several ethylsilanes and ethylgermanes on Si surfaces [25–35].

Hydrogen TPD results, obtained by mass spectrometry, can also yield quantitative information about the amount of Ge deposited on the Si(100) surface. The coverage of Ge on the surface is determined by relating the hydrogen atom coverage, measured by TPD, to the number of hydrogen atoms present per decomposing GeH₃Et molecule. The coverage calculation assumes the following overall reaction:



By integration of the number of desorbing H atoms and consideration of the mass balance, the amount of Ge deposited is determined. This reac-

tion does not depend on the actual surface species which are generated in the adsorption step. However, it does require that all the surface species created upon the adsorption of a GeH₃Et molecule remain bound to the surface. This condition was confirmed experimentally by checking for the desorption of species from the surface during the GeH₃Et exposure, and no desorption was observed. Careful calibration of the C₂H₄ signal was also used to double-check the Ge coverage results obtained by H₂ desorption.

The results of the Ge coverage determinations show that the amount of GeH₃Et which decomposes and deposits Ge reaches a constant value at long exposure times. The maximum amount of Ge which is deposited onto the Si(100) surface is $2.6 \times 10^{14} \text{ cm}^{-2}$ in a given adsorption cycle. This value is also confirmed by XPS. The Ge 2p_{3/2}/Si 2p peak ratios were also measured as a function of GeH₃Et coverage. The ratios were then compared to the same ratios determined for GeH₄ and Ge₂H₆ decomposition, where the coverage of Ge deposited was determined previously [55]. The coverage of Ge determined by XPS is in excellent agreement with the coverage determined by TPD. This agreement further indicates that the assumptions made in the use of Eq. (6) are justified.

The reaction shown in Eq. (6) shows that Ge is the only surface species remaining. The other two products of the reaction desorb as gases. XPS and AES spectra taken after a GeH₃Et exposure and a temperature ramp revealed a surface which was free from carbon contamination. The lack of carbon is an important observation for the possible growth of Ge films by this alternative precursor in a CVD environment. Also, the saturation behavior for the deposition of Ge from GeH₃Et indicates that this molecular precursor may be useful for atomic layer epitaxy applications.

The maximum amount of Ge which can be deposited from a saturation exposure of GeH₃Et is $2.6 \times 10^{14} \text{ Ge atoms per cm}^2$. In similar experiments using GeH₂Et₂ as a Ge-containing precursor, the maximum amount of Ge deposited was $1.7 \times 10^{14} \text{ Ge atoms per cm}^2$ [35]. Using GeH₂Et₃, the maximum amount of Ge deposited was $1.5 \times 10^{14} \text{ Ge atoms per cm}^2$ [56]. The trend in

this series of molecules is for the Ge coverage to decrease with an increasing number of ethyl ligands on the precursor molecule. This trend can be explained on the basis of site-blocking or steric considerations. Each of these Ge-containing molecules adsorbs dissociatively on Si(100), depositing ethyl groups and surface hydrides. The ethyl groups, due to their larger size, can block a larger number of adjacent Si sites than hydrogen atoms are able to block. This simple geometric consideration can explain the observed trend in the ethyl-germane series.

5. Conclusions

We have studied the surface chemistry of GeH₃Et on the Si(100)-(2 × 1) surface. This molecule adsorbs dissociatively at low coverages to yield adsorbed ethyl groups and hydrogen. As the surface is heated, the surface ethyl groups decompose by a hydride elimination reaction which evolves ethylene into the gas phase. The surface hydrogen atoms recombine above the ethylene desorption temperature and desorb as molecular hydrogen. Germanium is left at the surface after the desorption of ethylene and hydrogen. The maximum amount of Ge which can be deposited following a saturation exposure of GeH₃Et and desorption of H₂ and C₂H₄ is 2.6 × 10¹⁴ Ge atoms per cm², or 0.38 ML.

Acknowledgements

The authors are happy to acknowledge the National Science Foundation (Grant CHE-9100429) for support of this research. One of the authors (C.M.G.) also acknowledges the National Science Foundation for an NYI Award.

References

- [1] M.L. Green, D. Brasen, H. Temkin, R.D. Yadavish, T. Boone, L.C. Feldman, M. Geva, B.E. Spear, *Thin Solid Films* 184 (1990) 107.
- [2] S.S. Iyer, G.L. Patton, J.M.C. Stork, B.S. Meyerson, D.L. Harame, *IEEE Trans. Electron. Dev.* 36 (1989) 2043.
- [3] S.S. Iyer, G.L. Patton, D.L. Harame, J.M.C. Stork, E.F. Crabbé, B.S. Meyerson, *Thin Solid Films* 184 (1990) 153.
- [4] T.P. Pearsall, *CRC Crit. Rev. Solid State Mater. Sci.* 15 (1989) 551.
- [5] J. Welsler, J.L. Hoyt, J.F. Gibbons, *Jpn. J. Appl. Phys. Part 1* 33 (1994) 2419.
- [6] K. Werner, A. Strom, S. Butzke, J.M. Maes, M. van Rooy, P. Alkemade, E. Algra, M. Somers, B. de Lange, E. van der Drift, T. Zijlstra, S. Radelaar, *J. Crystal Growth* 164 (1996) 223.
- [7] G.L. Zhou, H. Morkoç, *Thin Solid Films* 231 (1993) 125.
- [8] P.D. Agnello, T.O. Sedgwick, M.S. Goorsky, J. Ott, T.S. Kuan, G. Scilla, *Appl. Phys. Lett.* 59 (1991) 1479.
- [9] M. Cao, A.W. Wang, K.C. Saraswat, *Proc. Electrochem. Soc.* 93 (1993) 350.
- [10] D. Dutartre, P. Warren, I. Berbezier, P. Perret, *Thin Solid Films* 222 (1992) 52.
- [11] P.M. Garone, J.C. Strum, P.V. Schwartz, *Appl. Phys. Lett.* 56 (1990) 1275.
- [12] S.M. Jang, R. Reif, *Appl. Phys. Lett.* 59 (1991) 3162.
- [13] T.I. Kamins, D.J. Meyer, *Appl. Phys. Lett.* 59 (1991) 178.
- [14] H. Kühne, T. Morgenstern, P. Zaumseil, D. Krüger, E. Bugiel, G. Ritter, *Thin Solid Films* 222 (1992) 34.
- [15] B.S. Meyerson, K.J. Uram, F.K. LeGoues, *Appl. Phys. Lett.* 53 (1988) 2555.
- [16] M. Racanelli, D.W. Greve, *Appl. Phys. Lett.* 56 (1990) 2524.
- [17] D.J. Robbins, J.L. Gasper, A.G. Cullis, W.Y. Leong, *J. Appl. Phys.* 69 (1991) 3729.
- [18] T.O. Sedgwick, P.D. Agnello, *J. Vac. Sci. Technol. A* 10 (1992) 1913.
- [19] M. Suemitsu, F. Hirose, N. Miyamoto, *J. Crystal Growth* 107 (1991) 1015.
- [20] Y. Zhong, M.C. Öztürk, D.T. Grider, J.J. Wortman, M.A. Littlejohn, *Appl. Phys. Lett.* 57 (1990) 2092.
- [21] B. Darlington, M. Foster, A. Champion, *Surf. Sci.* 304 (1994) L407.
- [22] J. Schmidt, C. Stuhlmann, H. Ibach, *Surf. Sci.* 302 (1994) 10.
- [23] D.A. Lapiano-Smith, F.J. Himpsel, L.J. Terminello, *Mater. Res. Soc. Symp. Proc.* 307 (1993) 155.
- [24] M. Foster, B. Darlington, J. Scharff, A. Champion, *Surf. Sci.* 315 (1994) L947.
- [25] A. Mahajan, B.K. Kellerman, N.M. Russell, S. Banerjee, A. Champion, J.G. Ekerdt, A. Tasch, J.M. White, D.J. Bonser, *J. Vac. Sci. Technol. A* 12 (1994) 2265.
- [26] A. Mahajan, B.K. Kellerman, J.M. Heitzinger, S. Banerjee, A. Tasch, J.M. White, J.G. Ekerdt, *J. Vac. Sci. Technol. A* 13 (1995) 1461.
- [27] P.A. Coon, M.L. Wise, A.C. Dillon, M.B. Robinson, S.M. George, *J. Vac. Sci. Technol. B* 10 (1992) 221.
- [28] A.C. Dillon, M.B. Robinson, M.Y. Han, S.M. George, *J. Electrochem. Soc.* 139 (1992) 537.
- [29] P.A. Coon, M.L. Wise, A.C. Dillon, S.M. George, *Mater. Res. Soc. Symp. Proc.* 282 (1993) 413.

- [30] A.C. Dillon, M.B. Robinson, S.M. George, Surf. Sci. 286 (1993) L535.
- [31] P.A. Coon, M.L. Wise, S.M. George, J. Chem. Phys. 98 (1993) 7485.
- [32] P.A. Coon, M.L. Wise, Z.H. Walker, S.M. George, D.A. Roberts, Appl. Phys. Lett. 60 (1992) 2002.
- [33] C.M. Greenlief, D.-A. Klug, L.A. Keeling, Mater. Res. Soc. Symp. Proc. 282 (1993) 427.
- [34] Y. Takahashi, H. Ishii, K. Fujinaga, J. Electrochem. Soc. 136 (1989) 1826.
- [35] W. Du, L.A. Keeling, C.M. Greenlief, J. Vac. Sci. Technol. A 12 (1994) 2281.
- [36] J.E. Griffiths, Inorg. Chem. 2 (1963) 375.
- [37] C.M. Greenlief, P.C. Wankum, D.-A. Klug, L.A. Keeling, J. Vac. Sci. Technol. 10 (1992) 2465.
- [38] M.J. Frisch, G.W. Trucks, M. Head-Gordon, P.M.W. Gil, M.W. Wong, J.B. Foresman, B.G. Johnson, H.B. Schlegel, M.A. Robb, E.S. Replogle, R. Gomperts, J.L. Andres, K. Raghavachari, J.S. Binkley, C. Gonzalez, R.L. Martin, D.J. Fox, D.J. Defrees, J. Baker, J.J.P. Stewart, J.A. Pople, Gaussian 92, Revision C, Gaussian Inc., Pittsburgh, PA, 1992.
- [39] P.J. Hay, W.R. Wadt, J. Chem. Phys. 82 (1985) 299.
- [40] P.J. Hay, W.R. Wadt, J. Chem. Phys. 82 (1985) 270.
- [41] W.R. Wadt, P.J. Hay, J. Chem. Phys. 82 (1985) 284.
- [42] J.A. Pople, R. Krishnan, H.B. Schlegel, J.S. Binkley, Int. J. Quantum Chem. Symp. 13 (1979) 225.
- [43] G. Beltram, T.P. Fehlner, K. Mochida, J.K. Kochi, J. Electron Spectrosc. Relat. Phenom. 18 (1980) 153.
- [44] T. Koopmans, Physica 1 (1933) 104.
- [45] W.L. Jorgensen, L. Salem, The Organic Chemist's Book of Orbitals, Academic Press, New York, 1973.
- [46] D.-A. Klug, C.M. Greenlief, J. Vac. Sci. Technol. A 14 (1996) 1826.
- [47] L.A. Keeling, L. Chen, C.M. Greenlief, A. Mahajan, D. Bonser, Chem. Phys. Lett. 217 (1994) 136.
- [48] G. Schulze, M. Henzler, Surf. Sci. 124 (1983) 336.
- [49] K. Fujiwara, Phys. Rev. B 26 (1982) 2036.
- [50] F.J. Himpsel, D.E. Eastman, J. Vac. Sci. Technol. 16 (1979) 1297.
- [51] T. Sakurai, H.D. Hangstrum, Phys. Rev. B 14 (1976) 1593.
- [52] F. Bozso, P. Avouris, Phys. Rev. B 38 (1988) 3943.
- [53] E. Landemark, C.J. Karlsson, L.S.O. Johansson, R.I.G. Uhrberg, Phys. Rev. B 49 (1994) 16523.
- [54] J.J. Koulmann, D. Steinmetz, F. Ringeisen, D. Bolmont, Physica B 170 (1991) 492.
- [55] D.-A. Klug, W. Du, C.M. Greenlief, J. Vac. Sci. Technol. A 11 (1993) 2067.
- [56] L.A. Keeling, Ph.D. thesis, University of Missouri, 1995.
- [57] D. Steinmetz, S. Van, F. Ringeisen, D. Bolmont, J.J. Koulmann, Surf. Sci. 269/270 (1992) 415.
- [58] L. Stauffer, S. Van, D. Bolmont, J.J. Koulmann, C. Minot, Surf. Sci. 307/308 (1994) 274.
- [59] S. Van, D. Steinmetz, F. Ringeisen, D. Bolmont, J.J. Koulman, Phys. Rev. B 44 (1991) 13807.
- [60] J. Chen, C.M. Greenlief, J. Vac. Sci. Technol. A 15 (1997) 1140.